CONF-890315--1

ADVANCED BATTERIES FOR ELECTRIC VEHICLES

Paul A. Nelson

Argonne National Laboratory
Chemical Technology Division
9700 South Cass Avenue
Argonne, Illinois 60439

CONF-890315--1

DE89 009771

ABSTRACT

Over the past twenty years, some of the most difficult problems have been solved in the development of long-lived lithium/sulfide secondary batteries having molten chloride electrolytes. Recent tests of Li-Al/FeS_2 cells have demonstrated 1000 cycles of operation and the practicality of achieving a specific energy of 175 Wh/kg for prismatic cells. Bipolar cells now under study may achieve even higher specific energy. Also, bipolar cells make possible the use of low-cost coated current collectors for the positive electrode instead of the expensive molybdenum current collectors that have been required for prismatic cells. Very compact batteries to power an electric van have been conceptually designed with this approach. These batteries would provide a range for the loaded vehicle of more than 100 miles for a battery weighing 280 kg, only 15% of the loaded vehicle weight (1930 kg).

Introduction

Batteries having molten-salt electrolytes are of interest because of the high ionic conductivity of molten salts and the feasibility of using lightweight reactive elements and alloying materials at the high temperatures and oxygen-free conditions appropriate for molten-salt electrolytes. Primary cells with molten-salt electrolytes have been developed for Li-Al/FeS_2, Li-Si/FeS_2, and Li-Al/FeS electrode combinations. In general, these primary cells are formed into bipolar stacks of very thin electrodes, providing high power and high specific energy for various military and space power applications. Secondary batteries having molten-salt electrolytes also have high specific energy and long cycle life as compared to rechargeable batteries having other types of electrolyte. Research and development work has been carried out on rechargeable batteries having (1) negative electrodes of lithium or lithium alloys and calcium or calcium alloys and (2) positive electrodes of tellurium, selenium, sulfur, and metal sulfides such as FeS, FeS_2, Ni_2S_3, NiS_2, CoS_2, and TiS_2. Molten halide electrolytes and separators of boron nitride fibers or magnesia powder have typically been used.

This paper considers Li-alloy/FeS and Li-alloy/FeS_2 cells and batteries being developed for the electric vehicle application under sponsorship by the Department of Energy and its predecessors.

Comparison of Battery Couples

Work on the Li/S cell with an electrolyte of LiCl-KCl (m.p., 352°C) was begun at Argonne National Laboratory in the late 1960s.(1) At the cell operating temperature of about 400°C, both of the electrodes of this system are molten, and serious problems arise because of (1) the escape of liquid lithium from the negative electrode, causing the cell to be short circuited, and (2) the high solubility of both sulfur and lithium in the electrolyte. The solutions for these problems, which were first introduced in the period 1972-1973, are the use of Li-Al or Li-Si negative electrodes and FeS or FeS_2 positive electrodes.(2,3) These electrode materials are solids at the operating temperature of the cell, and thus, their use avoids the problems of the liquid electrodes and makes practical cells possible. Also, the use of lithium alloys reduces the lithium activity from that of elemental lithium, and this made possible the use of boron nitride fiber separators.

The theoretical specific energies of the lithium/sulfide cells and the sodium/sulfur cell are compared in Table 1. It is apparent that the substitution of alloys and compounds for the elemental materials reduced the theoretical specific energy from about 2555 Wh/kg for the Li/S cell to 460 Wh/kg for the Li-Al/FeS cell and to 485 to 630 Wh/kg for the Li-Al/FeS_2 cell. The value for the latter cell depends on the extent of reaction of the positive electrode. Some examples of overall cell reactions are the following:

$$2\text{Li-Al} + \text{FeS} \rightarrow \text{Li}_2\text{S} + \text{Fe} + 2\text{Al} \qquad [1]$$

$$2\text{Li-Al} + \text{FeS}_2 \rightarrow \text{Li}_2\text{FeS}_2 + 2\text{Al} \qquad [2]$$

$$4\text{Li-Al} + \text{FeS}_2 \rightarrow 2\text{Li}_2\text{S} + \text{Fe} + 4\ \text{Al} \qquad [3]$$

TABLE 1. Specific Energies of Selected Cell Couples

System	Positive Electrode Discharge Product	Theoretical Specific Energy (Wh/kg)
Li/S	Li_2S	2555
Li-Al/FeS	Fe,Li_2S	460
Li-Al/FeS_2	Li_2FeS_2	485
Li-Al/FeS_2	Li_2S,Fe	630
$Li_{3.25}$-Si/FeS_2	Li_2S,Fe	885
Na/S	Na-$S_{1.5}$	760

The fraction of the theoretical specific energy that can be achieved for practical cells differs markedly for the couples shown in Table 1. The important factors are the voltages of the cells and the densities of the reactants and the discharge products. The densities of the materials have a surprisingly important effect on the achievable specific energy.(4) For instance, the third system shown in Table 1, Li-Al/FeS_2 discharged to Li_2FeS_2, has a theoretical specific energy of only 485 Wh/kg, but shows promise of achieving a higher actual specific energy than that of any of the other couples shown in the table because both FeS_2 and the reaction product have high densities (4.8 g/cm^3 and 3.0 g/cm^3, respectively) and, thus, small volumes. The small active material volumes in all states of charge result in the need for less electrolyte to fill the voids in comparison to other electrodes. Other cells on the list also have favorable attributes. For instance, the positive current collectors in Li-Al/FeS cells can be made of steel, whereas the disulfide-type cells require current collectors of molybdenum or other materials compatible with FeS_2 and chloride salts.

Cell Components

Most of the lithium/sulfide cells tested have had lithium-aluminum negative electrodes. The phase diagram for the Li-Al system is shown in Fig. 1, and the voltage for a Li-Al electrode as lithium is titrated into the alloy is shown in Fig. 2.(5) Usually, the operation of the Li-Al electrode takes place on the $\alpha+\beta$ voltage plateau (300 mV relative to lithium), which extends from about 8 atom % lithium to about 48 atom % lithium. The electrode can be operated in the β-phase region and in the $\beta+\gamma$ region, but the high lithium activity in these regions, as shown in Fig. 2, requires special care in the selection of the separator.

The lithium-silicon alloy electrode has a higher theoretical specific energy than Li-Al because silicon is light and will accept several atoms of lithium per atom of silicon, as shown in Table 2.(6,7,8) However, the use of silicon as an alloying agent for lithium is not as advantageous as it would first appear.(9) First, much of the lithium is not usable because it is released at too low an operating cell voltage. This additional lithium increases the volume of the electrode and is a cost penalty for the expensive unused lithium. Second, the rate of reaction for the Li-Si electrode is lower (particularly on the lowest voltage plateau) than that for Li-Al. Third, the lower density of Li-Si partially counteracts the lower weight of silicon by requiring more electrolyte in the more voluminous electrode. Finally, silicon is corrosive to the current collector; nickel may not be acceptable for Li-Si electrodes, whereas steel current collectors show negligible corrosion in contact with Li-Al. Improved design may result in the Li-Si alloy being favored over Li-Al, but in current designs, the Li-Al alloy appears to have a slight overall advantage in specific energy, power, and cost.

The discharge paths for FeS and FeS_2 electrodes are shown in Fig. 3.(8,9) The sulfide phases observed during charging of Li-Al/FeS_2 cells are shown in Table 3(10,11) and the voltage curve vs. capacity of a Li-Al/FeS_2 cell discharged at a low rate is shown in Fig. 4.(12) Experimental results and calculations of cell weight have indicated that the best combination of high power and high specific energy can be obtained in a practical Li-Al/FeS_2 cell by limiting the discharge to the "A," "B," and "C" reactions shown in Fig. 4, or only slightly beyond. Reaction on the "D" part of the discharge curve requires a larger Li-Al electrode and a higher volume fraction of electrolyte in the positive electrode to accommodate the low-density Li_2S formed on discharge on the "D" part of the curve. These larger weights coupled with the lower voltage for the "D" part of the curve result in a lower specific energy, low power near the end of the discharge, and the requirement for accommodation in the power conversion system of a large voltage drop on discharge. Therefore, recent experimental work has been confined to cells operating on the upper plateau of the voltage curve.(13)

The same type of separator may be used for either the FeS or FeS_2 cell because the separator requirements are mainly restricted by the high lithium activity in the negative electrodes. The initial choice of material, that of a boron nitride fiber, was first used in the form of a woven fabric and later as a non-woven felt.(14,15) The felt has good strength and is 70% open space when compressed. It has demonstrated long life of 1000 cycles of operation with Li-Al electrodes over a period of two years. However, it is difficult to remove all the oxygen from the BN fiber during manufacture, and as a result, the BN is attacked by lithium at high lithium activities near that of elemental lithium with formation of a conductive film.

Magnesia powder was later considered for the separator because it is more widely available and is less costly. It also has greater chemical stability in contact with lithium at high activity than BN fiber. An MgO powder separator with very high surface area provides a separator having plastic-like properties and 60 to 80 vol % molten salt. But cells having MgO powder separators must be operated in an electrolyte-starved state to avoid formation of a low-viscosity suspension of the MgO in the electrolyte, which would permit the electrodes to touch and form a short circuit. A composite of MgO powder/BN fiber structure is now being given consideration and may provide a good mix of physical and chemical properties.

The MgO powder separator is fabricated as a cold-pressed plaque containing finely ground electrolyte salt. These plaques have been made in rather large sizes of 12 x 17 cm sheets of 1 to 2 mm thickness. They are of sufficient strength for routine cell assembly. Separators of boron nitride felt sheets are handled similarly to the MgO powder plaques, but without incorporation of the electrolyte during forming. Boron nitride is not readily wetted by the molten salt, and the wetting treatment (surface deposition of MgO) transforms the BN felt into a stiff board-like material. The electrolyte is vacuum-infiltrated after cell assembly when BN felt is used, but no electrolyte is added in cells having MgO powder separators.

Cell Design

For the Li-alloy/FeS cells, the contemporary design is based on a rectangular plate-type electrode and a prismatic cell design for ease of cell assembly and compactness of the battery. Corrosion studies have indicated that both low carbon and stainless steel are suitable for the cell housing. Cell housings can be formed by welding sheet metal or stamped metal forms and by deep drawing. Internal parts such as current collectors, electrode encapsulations, and electrode facial sheets have been made from both low carbon steel and stainless steel.

The prismatic cell design requires only one electrical feedthrough since one set of electrodes, usually the negative set, is grounded to the cell housing. The feedthrough is composed of annular ceramic insulating components such as BeO, MgO, or BN, which are positioned around a rod-shaped electrical terminal of about 6 to 12 mm dia.

The multiplate Li-alloy/FeS cells consist of rectangular, vertically oriented electrodes having electrode bus bar connections welded together above the electrodes. The electrode faces have areas of 150 to 225 cm^2, with 15 x 15 cm and 12 x 18 cm being the most often used sizes.

The cell design that has been given most attention for the lithium/disulfide system is the prismatic cell with a double positive electrode at the center and two negative electrodes on each side. This simple design was selected because of limited resources. Some development would be required to fabricate a more complex current collector and bus bar system of molybdenum or coated materials that are resistant to attack by the positive electrode. At this time, the powder-packed feedthrough imposes restrictions upon the current-collector design. New feedthrough technology is expected to open up new design approaches for prismatic cells using molybdenum or coated current collectors.

Another cell design that has been given recent consideration is the bipolar design. That approach greatly reduces the weight of the cell and simplifies the current collector design for the positive electrode.

Cell Performance

At this stage, lithium-limited FeS cells with MgO powder separators (Westinghouse Oceanic Systems, Cleveland, Ohio) are generally perceived as being furthest along in development. The lithium-limited FeS cells have good power at 80% depth-of-discharge (DOD) and provide a useable capacity of about 235 Ah under driving profile testing at a specific energy of about 115 Wh/kg. The cycle life expectancy of these cells is about 400 deep discharge cycles. Another developer, Electrofuel of Canada, uses a BN fiber-based separator, sometimes with the addition of MgO powder and an electrolyte of LiCl-KCl. Less is known about the performance of these somewhat smaller cells, but cycle life is reported to be greater than 700 cycles.

For the Li-Al/FeS_2 cells, recent experiments at ANL have resulted in two important milestone achievements. First, a cell has been operated for over 1000 cycles with less than 20% decline in performance at conditions that are projected to provide a specific energy of 175 Wh/kg at a 4-h discharge rate and a specific power of 200 W/kg at 80% DOD for a full-scale cell.(13) Second, a modified lithium/disulfide cell has demonstrated overcharge tolerance at trickle-charge rates of 2 to 3 mA/cm^2, which is sufficient for charger equalization of battery cells.(16)

Two innovations in the Li-Al/FeS_2 cell have brought about important improvements in the performance and cycle life stability.(4) These are a new electrolyte, LiCl-LiBr-KBr (310°C m.p.), and a dense FeS_2 electrode operated only on the upper voltage plateau. The broad liquidus region for LiCl-LiBr-KBr enables outstanding FeS_2 electrode kinetics at 400°C, a temperature well below that of FeS thermodecomposition. The operation of the densely loaded FeS_2 electrode on only the upper voltage plateau of the FeS_2 electrode has resulted in approximately double the electrode utilization and power that were obtained in operation of two-plateau cells of the same theoretical capacity.

Overcharge and Overdischarge Protection

Overcharging of cells results in attack of the iron or molybdenum current collector. For an FeS_2 electrode having a molybdenum current collector, $MoCl_2$ is formed at a voltage relative to Li-Al of about 2.4 V. Normally, the charging is completed at 2.05 V. In the operation of monosulfide cells, overcharge (which would result in attack of the steel or nickel collectors in the positive electrode) has been avoided by an electronic mechanism which bypasses current of up to 3 A around cells that have reached full charge voltage. This requires a wire to each cell, and thus, is expensive and complex and results in an additional failure mechanism--the wire contacting any part of the metallic structure of the battery and forming a short circuit.

Another method of overcharge protection that ANL has begun to investigate involves use of a "lithium-shuttle" mechanism. This mechanism results in an increased rate of self-discharge of cells that are at full charge while cells below full charge continue to charge. The processes involved are lithium dissolution at the negative electrode, chemical diffusion of dissolved lithium through the electrolyte to the positive electrode, and release of electrons and lithium ions at the positive electrode. The concentration of lithium at the negative electrode is determined from the solubility of lithium in the electrolyte at the lithium activity associated with the electrochemical potential of the negative electrode.

In recent tests with a lithium-alloy electrode in molten LiF-LiCl-LiBr (22:31:47 mol %), appreciable self-discharge rates of 2 to 5 mA/cm^2 were obtained at about -200 mV vs. the Li-Al reference electrode.(16) This potential is safely above that for the deposition of a molten lithium-rich phase. In tests with lithium-alloy/FeS cells, a combination of overcharge capacity and extended tolerance of a trickle charge has been demonstrated. Cells have been operated for more than 200 cycles under these conditions without shorting across the MgO separator. An experimental 6-Ah cell of the composition Li-Al + 10 mol % $Li_5Al_5Fe_2$/LiF-LiCl-LiBr(MgO)/FeS was operated at 475°C by T. D. Kaun at ANL. When charged to 1.47 V cutoff, the cell exhibited 99^+% coulombic efficiency and a self-discharge rate of only 0.2 to 0.4 mA/cm^2. When charged to a cutoff voltage of 1.57 V, the coulombic efficiency was noticeably reduced to about 93%. In the overcharge state, the cell can be trickle charged at 3 mA/cm^2 for 4 to 8 h without polarization of the sulfide electrode. More recently, a similar overcharge tolerance (2 to 3 mA/cm^2) has been demonstrated for a 25-Ah cell that has a composition of LiAl + 10 mol % $Li_5Al_5Fe_2$/LiCl-LiBr-KBr (MgO)/FeS_2 and is operated at 400°C. As in the test with the FeS electrode cell, there was a 20-fold increase in self-discharge rate for the cell as it reached the higher voltage associated with the benign overcharge state. This cell operated with no loss of capacity for over 225 cycles with an overcharge of 5 to 10% on every tenth cycle.

With regard to overdischarge of the cell, the lithium/disulfide cells are more tolerant than sodium/sulfur cells. When cells in a battery finally begin to fail, laboratory results show that the failure mechanism is always by a gradual increase in the rate of cell self-discharge, which finally results in overdischarging, formation of an internal short circuit, and reduction of the voltage of the battery. This should in no way affect the performance of adjacent cells and would occur only for cells for which the self-discharge rate has become so large that the automatic overcharging of the battery will not maintain the charge for these cells relative to that of other cells.

Cell Reversal

As an internal short circuit forms in a failing Li-Al/sulfide cell, the cell undergoes a moderate voltage reversal in subsequent discharges due to I^2R losses. Small batteries of FeS cells have been operated at ANL with one or more failed cells without damaging the other cells. The voltage reversal would be expected to amount to about 0.2 to 1.0 V at the end of the discharge for each failed cell.

Projected Cell Performance

Researchers at ANL have used the results of the cell tests to project the performance of lithium/disulfide cells in both the bicell and bipolar configuration and to compare these results with those projected for multiplate and bipolar monosulfide cells. The results are summarized in Table 4. The capacity and power at the end of discharge (EOD) of the four types of lithium/sulfide cells in Table 4 were selected to be appropriate for the Eaton DSEP van being developed by Chrysler and Eaton in a program for the Electric and Hybrid Propulsion Division of the Department of Energy. The specific energy of the multiplate monosulfide cell is essentially that which has been already achieved in the laboratory, but the specific power assumes about a 50% improvement, which is expected to be achieved with thinner electrodes. The bipolar monosulfide calculations are based on the electrode performances used for the multiplate cells, with the weight of the cell calculated by adding the weight of individual parts. The bipolar monosulfide cell would be approximately 7-1/2 in. in diameter and have electrodes 7-in. in diameter. The performance of the disulfide bicell is based on results achieved in the laboratory for smaller cells, with the weight calculated from the individual components. The calculations for the disulfide bipolar cell were based on the monosulfide bipolar calculations, with substitution of parts as necessary for the disulfide conditions.

Projected Battery Performance

Table 5 gives the projected performance for batteries constructed for the Eaton DSEP van. These results are based on the projected cell performances of Table 4. The initial range of the vehicle with a new battery would be 125 miles. At the end of battery life it would be 100 miles. The energy storage required of the battery was adjusted for the total weight of the vehicle, including the battery, to achieve the desired vehicle range (Table 5). It should be noted that the vehicle weight is a function of the battery weight, being 1649 kg plus the battery weight. The power at the end of discharge and at the end of battery life is sufficient for accelerating the vehicle to 50 mph in 20 s. With new batteries for which the powers at the end of battery discharge are given in the table, the acceleration would be approximately 20% more rapid than at the end of life.

The number of parallel strings in the batteries varies from one for the monosulfide multiplate to three for the bipolar batteries. For the bipolar batteries, each string would be housed in a separate insulating container of approximately 10-in. O.D.

There is a considerable difference among the batteries in total weight and volume. The disulfide bipolar battery, including the insulated housing, would have a specific energy of 167 Wh/kg. Part of this outstanding performance is due to the small volume and high density of the cells, and thus, to the light weight of the battery jacket. If, for instance, the cells of the disulfide bipolar battery were inserted in the jacket of the monosulfide multiplate battery, the specific energy of the total battery would decrease from 167 Wh/kg to 119 Wh/kg. It is seen that the volume of the cells, and thus, the internal volume of the jacket have a significant effect on the jacket weight and the overall battery weight.

To achieve equal thermal performance for a battery of high volume, it would be necessary to make a very thick insulating jacket. This is reflected in the higher rate of heat loss allowed for the multiplate monosulfide battery compared with the more compact batteries in Table 5. The monosulfide batteries would operate between about 440°C and 490°C, providing ample opportunity for thermal energy storage. The disulfide batteries would operate between 390°C and 440°C and would have an added advantage in that entropic cooling takes place on discharging the battery. This is illustrated in the diagram of Fig. 5. The entropic cooling effect more than counteracts the I^2R heating effect up to a current density of about 0.5 A/cm^2. Entropic heating need be dealt with only on charging of the battery, which may be carried out at a low rate over a period of 8 to 15 hours. Thus, the cooling requirements for the lithium/disulfide battery are less than for any other high-temperature battery.

Although the DSEP van would have the same performance with all four batteries in terms of range and acceleration, the analysis of Table 5 is not a fair comparison of the batteries; it is strongly biased against the lighter batteries. The vehicles equipped with the disulfide bipolar battery would have the highest load-carrying capacity. Alternatively, the vehicles could be designed for the same overall mission (range, acceleration, and load-carrying capacity), in which case the vehicles with batteries of the highest specific energy would have lighter chassis, tires, motors, and controllers and, thus, would require batteries of even smaller capacity than those shown in Table 5 for the lightweight batteries. This would result in a substantial cost savings. Also, the energy use would be less for the lightweight batteries and vehicles. The bipolar Li-Al/FeS_2 battery would provide a range for the loaded vehicle of more than 100 miles (125 miles initially) for a battery weighing 280 kg, only 15% of the loaded vehicle weight of 1929 kg.

Reliability and Life

Tests of FeS batteries of up to 27 cells have indicated that the reliability of the battery should be excellent, and its life may be only slightly less than that of the cells. This conclusion is reached because the malfunction of a cell seldom causes propagation of failure to other cells. Because of the use of long series-connected strings, the failures of single cells, which always result in the short-circuit condition, do not influence the operation of other cells in the string and only reduce the total voltage of the string. This situation can be planned for in the design of the battery. The operation of Li-Al/FeS cells, for which there are more data than for the Li-Al/FeS_2 system, indicates that the cell failure distribution has a very steep Weibull slope. Thus, the failure of 10% of the cells will occur only

50 to 100 cycles prior to the failure of the cell of median-lifetime cell in the battery. It is expected that a mature Li-Al/FeS_2 battery would behave in a similar manner.

As noted above, in recent tests with lithium/disulfide cells, several cells have operated for more than 1000 cycles. In earlier work, the brief lifetime of lithium/disulfide cells was a serious problem. Cell failure was apparently due to the transfer of iron and polysulfide ions through the electrolyte into the separator, where they precipitated on reaction with dissolved lithium, resulting in removal of capacity from the positive electrode and short circuiting of the cell. This has been solved primarily by utilization of the LiCl-LiBr-KBr electrolyte (320°C m.p.), which permits operation of the cell at 400°C to 450°C.

The battery designs of Table 5 could accept considerable reduction in stored energy and power toward the end of their lives, but still deliver the required energy for the design range (100 miles) and the power needed for the design acceleration. Under these circumstances, several failed cells undergoing voltage reversal (perhaps 10% of the total) could be tolerated.

It appears reasonable to assume that a life of 1000 equivalent full cycles can be achieved in a complete lithium/disulfide battery, and that this should be sufficient for several years of vehicle operation over a total distance in excess of 100,000 miles.

Scaleup

The operation of prismatic Li-Al/FeS cells with the capacities shown in Table 4 has already been demonstrated, and operation of cells of about one-third the indicated capacity has been achieved for the Li-Al/FeS_2 system. Based on these results, there appears to be no limitation in scaling up prismatic cells to the full size required for the Eaton DSEP van batteries. There is little experience in testing bipolar cells of either type, but, within the ranges shown in Table 4, the capacity of the cells and battery would not appear to be a limitation.

Advantages and Limitations

The most obvious fundamental advantage of the disulfide battery for vehicle applications is its outstanding specific energy and specific power in a complete battery package, including the insulating jacket. If the disulfide system meets its full potential in this regard, it would be difficult for any other system to match this performance. Also, the battery cells reliably establish a short circuit on failure. This greatly eases battery design and makes it possible to place many cells in series connection and to operate a battery with as many as 10% of the cells in the failure mode. The battery has excellent thermal performance, as noted above, and virtually no penalty in energy efficiency is expected for maintaining the temperature of the battery. Cooling should be required only during charging for the disulfide type of battery.

For the disulfide cell, the materials cost for the lithium and for the positive current collector warrant development work. Some work has been done on fabricating cells in the fully uncharged condition. This would mean fabricating the disulfide cell with a mixture of FeS and Li_2S in the positive electrode and a porous aluminum plaque in the negative electrode. This would be desirable because Li_2S is expected to be considerably less expensive than Li-Al. It is recognized that some substitute should be found for the molybdenum current collectors of the positive electrodes that have been used in research cells in the laboratory. Molybdenum may be too expensive and too difficult to fabricate for low-priced cells. Clever design may permit the use of base metal current collectors coated with molybdenum, molybdenum carbide, titanium nitride, or yet untested coatings. All of these coatings have been given consideration, and some have been given limited testing, but the best solution can be found only with a fairly intensive program involving both cell design and testing of coatings.

The disulfide batteries are expected to have outstanding reliability and safety characteristics. The system has intrinsic properties that make it safe in operation both during normal and accident conditions. The electrodes are solid materials that are completely saturated with a nonflammable molten salt, which excludes the air environment even if the cells are broken open and the contents are exposed to air. This was once done for monosulfide cells in a deliberate experiment. The operation of the cells does not generate gases, e.g., hydrogen, and the cell is completely sealed within a strong metal cell container, which, in turn, is sealed within a double-walled insulating jacket containing an inert gas.

The most outstanding performance will be achieved with development of disulfide bipolar batteries. Such batteries would incorporate reliable chemical overcharge protection within the cells, a low-cost coating on the positive side of the bipolar cell plate, and a hermetic sealant around the edge of the cell between the positive and negative electrodes. Also, required are clever designs which simplify the means of fabricating the seal between the two electrodes, loading the electrodes into the cells, and edge-welding each cell in a completed stack. ANL has initiated experimental work to show the viability of these designs.

Acknowledgment

The author thanks T. D. Kaun for his technical review and correction of this paper and J. E. Harmon for editorial review. Most of the work discussed was funded by Conservation and Renewable Energy, Department of Energy.

References

1. E. J. Cairns and R. K. Steunenberg, "High Temperature Batteries," in **Progress in High Temperature Physics and Chemistry,** Vol. 5, C. Rouse, Ed., Pergamon Press, New York, 1973.

2. D. R. Vissers, Z. Tomczuk, and R. K. Steunenberg, **J. Electrochem. Soc., 121,** 655 (1974).

3. J. Birk and R. K. Steunenberg, "Chemical Investigations of Lithium-Sulfur Cells," in **New Uses of Sulfur,** J. R. West, Ed., Adv. Chem. Ser. 140, ACS, Washington, DC, pp. 186-202, 1975.

4. T. D. Kaun, **J. Electrochem. Soc., 132,** 3063 (1985).

5. C. J. Wen, B. A. Boukamp, R. A. Huggins, and W. Weppner, **J. Electrochem. Soc., 126,** 2258 (1979).

6. C. J. Wen and R. A. Huggins, **J. Solid State Chem., 37,** 271 (1981).

7. H. G. V. Schnering, R. Nesper, K. F. Tebbe, and J. Curda, **Z. Met. 71,** 357 (1980).

8. D. R. Vissers et al., Chapter 10 in **"Lithium,"** O. Bock, Ed., John Wiley & Sons, New York, 1985.

9. T. D. Kaun, L. Redey, and P. A. Nelson, "Molten-Salt Battery Advances," **Proc. of 22nd IECEC,** Philadelphia, PA, pp. 1085-1090, (1987).

10. A. E. Martin, in "High Performance Batteries for Electric-Vehicle Propulsion and Stationary Energy Storage," **Argonne Nat. Lab. Rep. ANL-78-84,** p. 167, 1980.

11. A. E. Martin and Z. Tomczuk, in "High-Performance Batteries for Electric-Vehicle Propulsion and Stationary Energy Storage," **Argonne Nat. Lab. Rep. ANL-79-39,** pp. 71-73, 1979.

12. Z. Tomczuk, B. Tani, N. C. Otto, M. F. Roche, and D. R. Vissers, **J. Electrochem. Soc., 129,** 925 (1982).

13. T. D. Kaun, T. F. Holifield, and W. H. DeLuca, "Lithium Disulfide Cells Capable of Long Cycle Life," **Ext. Abstracts, 174th ECS Meeting,** p. 71, Chicago, IL, (Oct. 1988).

14. J. A. Smaga, F. C. Mrazek, K. M. Myles, and J. E. Battles, "Materials Requirements in LiAl/LiCl-KCl/FeS_x Secondary Batteries," in **Corrosion/78,** N. J. Hoffman and G. A. Whitlow, Eds., NACE, pp. 652-674, 1978.

15. R. B. Swaroop, J. E. Battles, and R. S. Hamilton, "Development and Evaluation of BN Felt as Separator Material," in **Proc. of the Sixth Inter-American Conf. on Materials Technology,** San Francisco, CA, August 12-15, 1980, pp. 67-71 (1980).

16. T. D. Kaun, T. F. Holifield, M. N. Nigohosian, and P. A. Nelson, "Development of Overcharge Tolerance in Li/FeS and $LiFeS_2$ Cells," **Ext. Abstracts, 174th ECS Meeting,** Vol. 88-21, p. 67, Chicago, IL, (Oct. 1988).

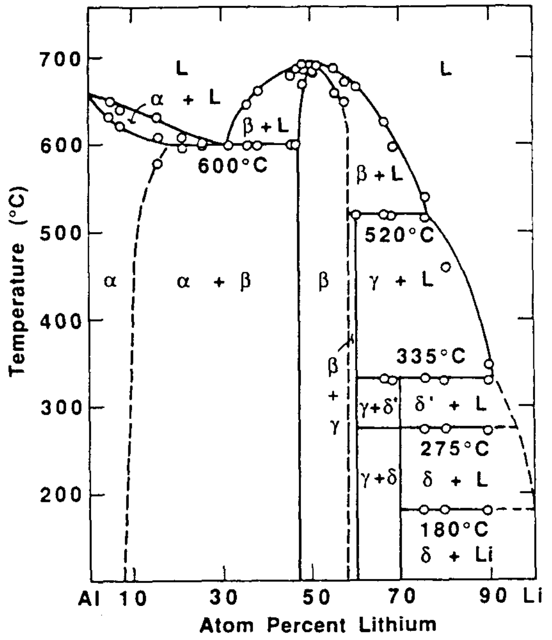

FIG. 1. Li-Al PHASE DIAGRAM

DISCLAIMER

Wen, Baukamp, Huggins, and Weppner, J. Electrochem. Soc. 126, 2258 (1979)

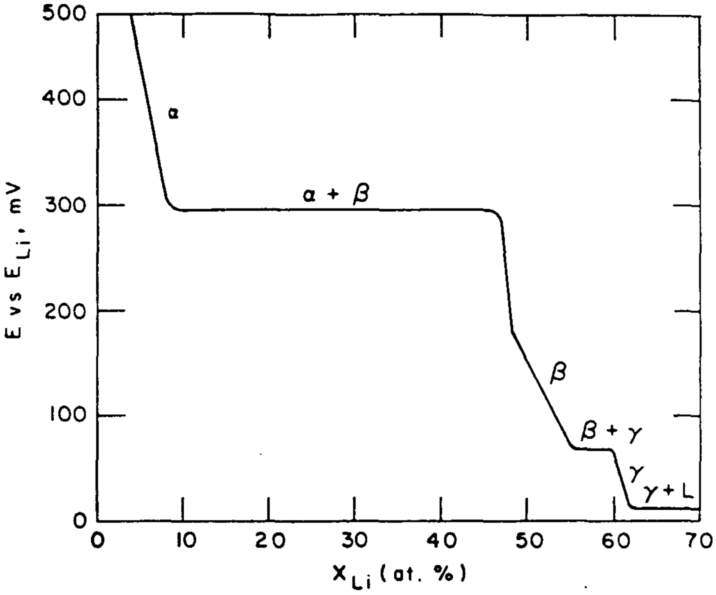

FIG. 2. COULOMETRIC TITRATION CURVE FOR LITHIUM-ALUMINUM SYSTEM AT 423°C

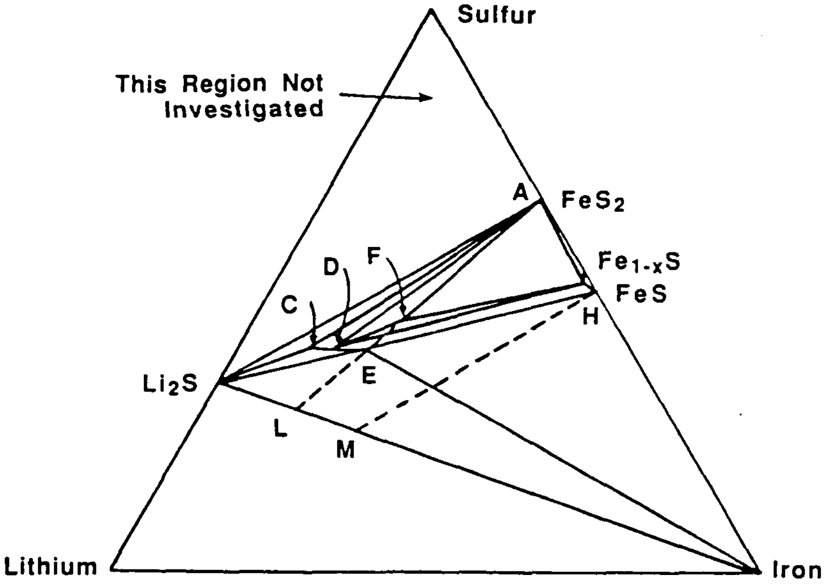

A-L = Discharge Path of FeS$_2$ Electrode
F = Li$_3$Fe$_2$S$_4$
C-D-E = Li$_{2+x}$Fe$_{1-x}$S$_2$
H-M = Discharge Path of FeS Electrode

FIG. 3. PHASES IN THE Li-Fe-S SYSTEM AT 450°C

Electrolyte: LiCl-KCl Eutectic
Temperature: 417°C
Current Density: 12 mA/cm^2

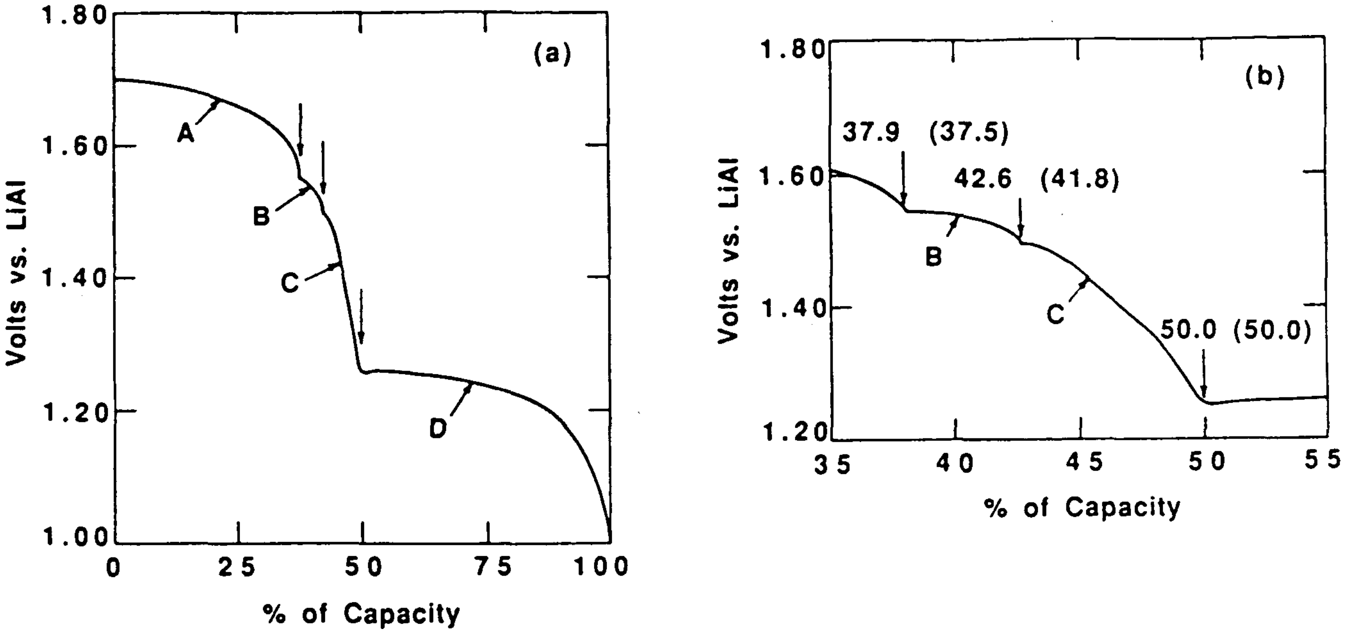

$$FeS_2 \xrightarrow{A} Li_3Fe_2S_4 \xrightarrow{B} Li_{2-x}Fe_{1-x}S_2 + Fe_{1-x}S \xrightarrow{C} Li_2FeS_2 \xrightarrow{D} Li_2S + Fe$$

FIG. 4. DISCHARGE CURVE FOR LiAl/FeS$_2$ CELL

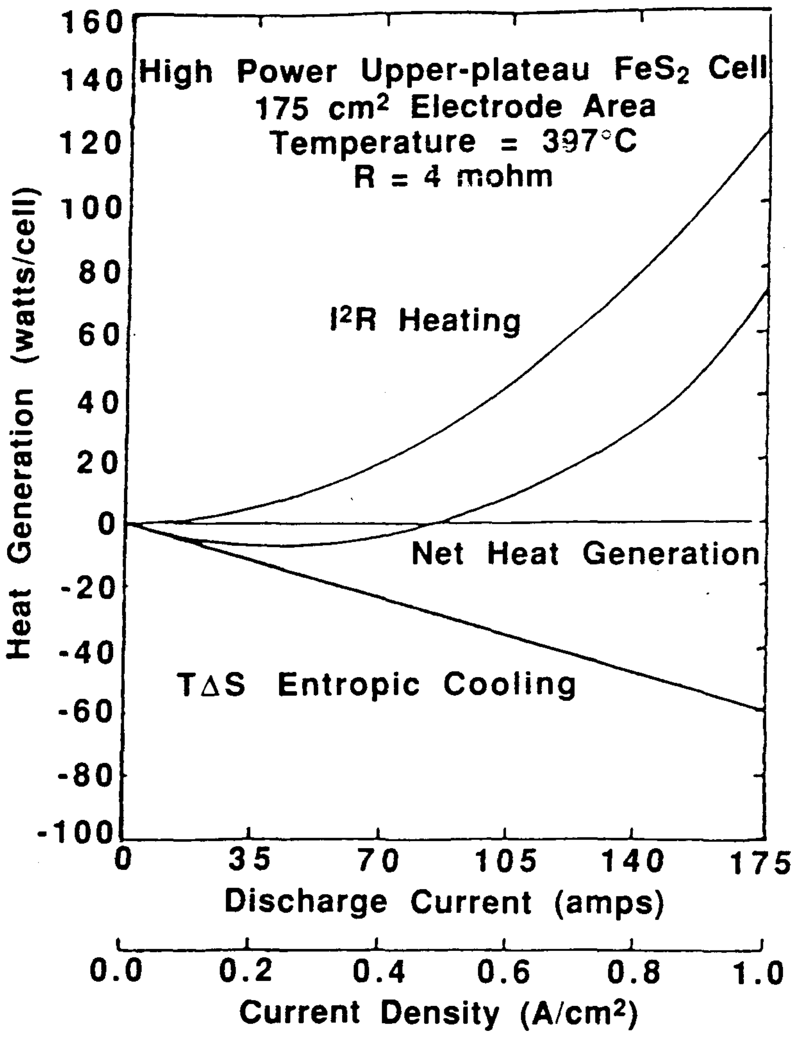

FIG. 5. DESIGN FOR ISOTHERMAL OPERATION

TABLE 2. CHARACTERISTICS OF Li-Si ALLOY ELECTRODE

Plateau Voltage Observed (mV)	Proposed Phase Transition		Lithium Reacted (ΔLi/Si)	
	Wen & Huggins	Max Planck	Wen & Huggins	Max Planck
-250	$Li_{4.41}Si \rightarrow Li_{3.317}Si$	$Li_{3.85}Si \rightarrow Li_{3.25}Si$	1.09	0.65
-142	$Li_{3.317}Si \rightarrow Li_{2.367}Si$	$Li_{3.25}Si \rightarrow Li_{2.33}Si$	0.95	0.92
-15	$Li_{2.367}Si \rightarrow Li_{1.731}Si$	$Li_{2.33}Si \rightarrow Li_{1.71}Si$	0.64	0.62
+34	$Li_{1.731}Si \rightarrow Si$	$Li_{1.71}Si \rightarrow Si$	1.73	1.71

At 450°C vs. Li-Al ($\alpha + \beta$).

TABLE 3. SULFIDE PHASES OBSERVED DURING CHARGE OF LiAl/FeS_2 CELLS OPERATED AT 410°C USING EUTECTIC ELECTROLYTE[a]

Charge Potential[b] vs. ($\alpha + \beta$) LiAl	X-Ray Findings		Metallographic Findings
	Major Phase	Minor Phase	
1.53	Li_2FeS_2	$LiK_6Fe_{24}S_{26}Cl$	Li_2FeS_2 + trace of $LiK_6Fe_{24}S_{26}Cl$
1.64	$Li_{2.33}Fe_{0.067}S_2$ and Li_2FeS_2	$Fe_{1-x}S$	$Li_2FeS_2 + Fe_{1-x}S + Li_{2.23}Fe_{0.67}S_2$
1.72	$Li_3Fe_2S_4$	None Detected	$Li_3Fe_2S_4$ Only
1.79	$Li_3Fe_2S_4$	None Detected	$Li_3Fe_2S_4$ + 5% $Fe_{1-x}S$
1.82	$Li_3Fe_2S_4$	$FeS_2 + Fe_{1-x}S$	Not Examined
1.85	FeS_2	$Fe_{1-x}S$	$Fe_2S + Fe_{1-x}S$

[a] Li_2S and Fe react at lower potential (1.33 V) to form Li_2FeS_2.

[b] Constant current charge at ~18 mA/cm^2 followed by >18-h constant voltage charge (final current density <2 mA/cm^2).

TABLE 4. LITHIUM/SULFIDE CELLS--PROJECTED PERFORMANCE

Based on Eaton DSEP Van Requirements

Characteristic	Monosulfide Multiplate	Monosulfide Bipolar	Disulfide Bicell	Disulfide Bipolar
Capacity, Ah	313	92	137	87
Specific Energy, Wh/kg	112	160	175	210
Specific Power at EOD, W/kg	127	182	199	239
Weight, g	3410	686	1250	663
Volume, cm^3	1310	250	455	240

TABLE 5. LITHIUM/SULFIDE VAN BATTERIES--PROJECTED PERFORMANCE

Basis: Eaton DSEP Van
Vehicle Weight: Base, 1376 kg; load, 273 kg; total, 1649 kg + battery weight
Range: 125 miles (range at end of battery life: 100 miles)
Energy Usage: 0.194 Wh/tonne-mile (FUDS cycle)
Power Requirement (end of discharge, end of battery life): 23 kW/tonne (0-50 mph/20 s)
Electronic Control: 400 A max, 200 V max open-circuit voltage

Characteristic	Monosulfide Multiplate	Monosulfide Bipolar	Disulfide Bicell	Disulfide Bipolar
Cells per Battery	150	450	224	336
Number of Parallel Strings	1	3	2	3
Capacity (FUDS Cycle), kWh	56.4	49.4	49.0	46.8
Power at EOD,[a] kW	64	56.3	55.7	53.3
Specific Energy, Wh/kg	83	127	132	167
Specific Power, W/kg	94	144	151	190
Weight, kg	680	390	370	280
Cell Fraction of Battery Wt	0.75	0.80	0.75	0.80
Volume, L	415	227	225	163
Dimensions, in.	59Lx43Wx10H	59Lx10D(3)[b]	42Lx33Wx10H	42Lx10D(3)[b]
Rate of Heat Loss, W	300	200	200	200

---

[a] 20% additional power over requirement is provided for new batteries to allow for battery degradation.

[b] Dimensions shown are for each of three modules.